

# Fuzzy Cognitive Map to Classify Plantar Foot Alterations

Julian Andres Ramirez-Bautista, Silvia L. Chaparro-Cárdenas, Antonio Hernández-Zavala, Ruth Magdalena Gallegos-Torres, Martha Zequera, Yosabad Tovar-Barrera, Juan M. Pradilla-Gómez and Jorge Adalberto Huerta-Ruelas

**Abstract**— The function of the back, hip, knee, ankle and other orthopedic alterations of the human body can be analyzed through plantar pressure distribution. The development of Clinical Decision Support Systems (CDSS) can handle the uncertainties present in biological data using different Artificial Intelligence techniques to obtain accurate and easy to use systems. This paper presents the application of a Fuzzy Cognitive Map (FCM) formulation, for knowledge extraction in the classification of human plantar foot alterations, with a relatively small and transparent model. The FCM is trained using the Bacterial Search Optimization Algorithm (BFOA). One hundred and twenty-five volunteer subjects (aged 20-68 years) participated in the study. Classification of the foot into normal (n=31), flat (n=32), cavus type III (n=31) and cavus type IV (n=31) to train the system was performed by specialized physicians. The test was performed by walking on a FreeMed® platform. The proposed method shows an accuracy rate of about 89% in the classification task and allows extracting information related to the important factors that the system considers to make a decision.

**Index Terms**— Clinical decision support systems, bacterial foraging optimization algorithm, fuzzy cognitive maps, optimization algorithms, plantar data analysis.

## I. INTRODUCTION

Currently there are large amounts of biomedical data with potential application in improving the quality of people life, since using effective and efficient computational knowledge systems, it is possible to include treatment recommendations, and prescribe preventive health tasks. But due to its complex nature, comprehensive techniques are required to model the relationship between data elements [1]–[3].

J. A. Ramirez, and S. L. Chaparro are with the Research Department of Fundación Universitaria de San Gil – UNISANGIL, km2 vía San Gil-Charalá, Santander, Colombia, jramirez@unisangil.edu.co; schaparro@unisangil.edu.co

A. Hernández-Zavala, and J. A. Huerta-Ruelas are with Centro de Investigación en Ciencia Aplicada y Tecnología Avanzada – Instituto Politécnico Nacional, Av. Cerro Blanco #141, Col. Colinas del Cimatario, Querétaro, México, anhernandez@ipn.mx; jhuertar@ipn.mx

R. M. Gallegos-Torres is with the Department of Nursing, Universidad Autónoma de Querétaro, Centro Universitario, 76010, Querétaro, México, isisrmgx@gmail.com.

M. Zequera is with the Electronic Department, BASPI-FootLaB, Pontificia Universidad Javeriana, Cra. 7 No. 40-62, Bogotá, Colombia, mzequera@javeriana.edu.co.

Y. Tovar-Barrera is with Yosafisio Clinic of Querétaro, México, yosafisiotb@outlook.com.

J. M. Pradilla-Gómez is with the School of Medicine, Pontificia Universidad Javeriana, Cra 7 No. 40–62, Bogotá, Colombia, juan\_pra\_28@hotmail.com

people life, since using effective and efficient computational knowledge systems, it is possible to include treatment recommendations, and prescribe preventive health tasks. But due to its complex nature, comprehensive techniques are required to model the relationship between data elements [1]–[3].

In the biomedical field, plantar pressure through static and dynamic measurements allows understanding the mechanical behavior of the human body to detect, monitor and treat many other diseases that are reflected in an abnormal distribution of plantar pressure. Abnormal foot posture (flat foot or cavus foot) has been associated with lower limb injuries, such as patellofemoral joint pain, medial tibial stress syndrome, Achilles tendinopathy, patellar tendinopathy, plantar fasciitis, medial midfoot arthritis, and posterior tibial tendon dysfunction [4].

Devices to measure plantar pressure under dynamic and static conditions may be divided into two groups: baropodometric platforms and instrumented insoles, which provide much information to identify patterns and correlate with medical conditions [5].

Specialized physicians are in charge of analyzing orthopedic alterations of the foot, but assessing the type of alteration based on the acquired data is a subjective judgment, being evident the development of classification algorithms [6]. However, this analysis requires easily interpretable systems with efficient techniques to deal with the inaccuracy, vagueness, and uncertainty present in medical and biological data due to the interpretation of information [7], [8].

Different studies have been reported in this field [9]–[11], Chae et al. have developed a deep learning model to classify foot deformity types according to image pressure data and numerical data [6]. Likewise, using one-dimensional convolutional neural networks and plantar pressure images obtained with instrumented insoles, they obtained a classification of normal, cavus and flat feet of 99.26% [12]. Li *et al.* proposed a Deep Neural Network model called resident network-based conditional generative adversarial nets (RNcGAN) to classify normal, flat, and talipes equinovarus feet, based on images achieving an accuracy of 95.17% [13].

Traditional classifiers, such as neural networks, have prediction rates greater than 90%, but they are considered black boxes, being a limitation because it makes the interpretation of the results difficult [14], since medical ethics require physicians to understand the fundamental inner workings of the devices in the

environment. [15]. Fuzzy cognitive maps (FCM), considered as an effective and robust artificial intelligence technique for modeling complex systems, have proven to overcome these difficulties, being a useful tool for designing knowledge-based systems that behave like human reasoning, giving interpretability to their network [16]. An FCM allows relating input concepts to output concepts by means of a graph that, although similar to that of an ANN, does not make use of complex activation functions [17]. Different proposals have been reported for the computation of the Fuzzy Cognitive Maps rule [18]–[20], in addition to being used for modeling complex systems, including medical decision support systems [8], [21]–[24]. Several authors have reported work with high accuracy rates using FCM [25], [26], such as the classification of flat and cavus foot using an FCM trained by Genetic Algorithm, reported by [27], reaching an accuracy of 91%.

This study applies an FCM formulation to extract knowledge about the classification of human plantar foot alterations. If the behavior of the FCM to obtain an expected result is known, it is possible to extract the most relevant factors that the algorithm considered to make the decision. The study supports the development of algorithms that not only have high-performance rates, but also transparent, to provide efficient feedback to the physician. The FCM is trained using the Bacterial Foraging Optimization Algorithm (BFOA) and historical data from 125 participating subjects with normal, flat, cavus type 3 and cavus type 4 foot, obtained for the presented study and classified by qualified physicians. The classification result was compared with previous authors and the classification performed by a group of physicians. Proposed methodology shows a better performance, with a relatively small and potentially transparent model.

## II. DATA PREPARATION

### A. Dataset

Foot plantar pressure data were acquired from 125 subjects with normal ( $n = 31$ ), cavus type 3 ( $n = 31$ ), cavus type 4 ( $n = 31$ ) and flat feet ( $n = 32$ ) for use in the classification system. The subjects participating in this study were 44% female and 56% male. All participants were informed of the purposes of the study and informed consent was written. The ethical standards established in the Declaration of Helsinki were considered. Additionally, the project with number SIP20196297 was approved by Instituto Politécnico Nacional (IPN) of México, which requires fulfill ethical requirements agreement. The inclusion criteria were men and woman with age between 20 to 68 years-old, height between 150 to 180 cm, weight between 46.4 to 103 kg, with a body mass index (BMI) between 18.5 and 24.9, a range of participants within normal healthy weight values. Exclusion criteria were people using support accessories (crutches, canes, etc.), lower extremity or foot surgeries, pregnancy, obesity, skeletal pathologies diagnosed in the lower limbs (referred by the participants) or an altered gait due to another disease.

The baropodographic platform was provided by the PIEDICA center in Mexico City, which has FreeMed® platforms with an

XY resolution of 2.5 dpi and an 8-bit Z resolution. During the experiment the participants recorded stepping cycles, each one with three steps taken continuously. The participants walked on a 6-meter surface with no slope, where the electronic acquisition platform was at the center of the walking surface. In this way, 3 trials per participant were acquired, and the percentage load data per unit area of interest were averaged, to obtain an unbiased measure representing the participant's plantar pressure distribution during normal walking.

### B. Fuzzy Cognitive Map (FCM)

Kosko proposed the FCM in 1986 to describe the relationships between the main variables (concepts) of a system and its behavior [28]. These values are represented by concepts ( $C$ ) interconnected by weights ( $W_{ji}$ ) that denote an increase/decrease of cause and effect in the concepts. A positive relationship ( $W_{ji}$ ) exists in the concepts ( $C$ ) when an increase in one concept causes an increase in the other concept. Otherwise, a negative relationship ( $W_{ji}$ ) exists when a particular concept causes a decrease in the next concept. When there is no relationship in the concepts, it is denoted as 0 [14], [29], [30].

To compute the state vector of the FCM in the next iteration, (1) is used.

$$x_i(t) = f\left(\sum_{j \neq i}^n x_j(t-1) W_{ji}\right) \quad (1)$$

Where  $x_i(t)$  is the current state of the concepts,  $W_{ji}$  is the weight matrix representing the relationship in the concepts,  $x_j(t-1)$  is the value of concept  $C_j$  at time  $t-1$  and  $f$  is the threshold function (2) used to keep the activation values in the range [0-1] [31].

$$f = \frac{1}{1+e^{-\lambda x}} \quad (2)$$

Where  $\lambda$  defines the steepness of the function and  $x$  refers to (1).

Self-connections are not allowed in the original Kosko model, but to use the self-memory feature, this condition was removed [31]. Similar formulation is proposed by [18], in which the previous value of each concept is considered. Thus, the new concept value is calculated through the multiplication of a portion to the state vector and the weight matrix, and the addition of a portion of the previous concept value. This formulation is represented by (3) [18].

$$x_i(t) = f\left[k_1 \sum_{j \neq i}^n x_j(t-1) W_{ji} + k_2 x_i(t-1)\right] \quad (3)$$

Where  $k_1$  expresses the [0-1] influence of the new value on the interconnected concepts,  $k_2$  is the [0-1] portion of the previous concept considered and  $x_i(t-1)$  are the values of the  $C_i$  concept at time  $t-1$ . Initially,  $k_1$  is set with a higher value, and  $k_2$  is set with a lower value, but during the FCM training process both parameters vary depending on the simulated system [18]. The inference rules are applied in the number of iteration needed until any of the stopping criteria is satisfied [32]. These criteria are: a) when the FCM simulation reaches a fixed-point attractor, the system is at an equilibrium point; b) the FCM simulation is at a limited cycle when a number of states behave

with a certain pattern; and finally, c) the FCM simulation may have a chaotic behavior. In either approach, the weight matrix will be based on expert knowledge or computed by learning algorithms and historical data [33], [34]. The most relevant approaches are Hebbian-based, population-based and hybrid learning. Hebbian-based methods consider the modified Hebbian law in the unsupervised learning process, adjusting the initial weights given by the experts in each iteration until the desired value is reached [35], [36]. Population-based algorithms substitute expert knowledge using optimization algorithms and historical input data. In the supervised process, the system is trained as a neural network until the minimum or maximum value of a cost function is reached [33], [37]. Hybrid approaches combine both types of learning to improve system performance [33].

### C. Bacterial Foraging Optimization Algorithm (BFOA)

BFOA was proposed by Kevin Passino (2002) to solve numerical optimization problems [38]. This technique is based on mimicking the foraging behavior of *E. coli* bacteria and has demonstrated competitive performance against well-known nature inspired optimization algorithms [39], [40]. The key idea of BFOA is the application of group foraging strategy of a swarm of *Escherichia coli* bacteria to optimize a multi-optimal function. The bacteria forage for nutrients in a way that maximizes the energy obtained per unit time. There are four main phases in BFOA [41], [42]:

**Chemotaxis:** This process simulates the movements of an *E. coli* cell through swimming and tumbling via flagella. A bacterium may swim for a period in the same direction or it may tumble, and alternate between these two modes of operation throughout its life. In computational chemotaxis, the movement of bacterium may be represented by (4).

$$\theta^i(j+1, k, l) = \theta^i(j, k, l) + c(i) \frac{\Delta(i)}{\sqrt{\Delta^T(i) \cdot \Delta(i)}} \quad (4)$$

Where  $\Delta$  is a vector in the random direction whose elements are in  $[-1, 1]$ ,  $j$ -th is the chemotactic step,  $k$ -th is the reproduction step,  $l$ -th is the elimination-dispersal step,  $\theta_i(j, k, l)$  is the  $i$ -th bacterium at  $j$ -th chemotactic and  $c(i)$  is the size of the step.

**Swarming:** The cell with the best environment sends signal to attract others, forming a swarm.

**Reproduction:** Less healthy bacteria die, while the healthier bacteria divide asexually into two bacteria. These are placed in the same location. This keeps the size of the swarm constant.

**Elimination and dispersal:** some bacteria are randomly liquidated with a very small probability, while new replacements are randomly initialized in the search space.

## III. MATERIALS AND METHODS

The use of each resolution point as a concept in the FCM makes the graph complex. To avoid this condition, the division of the foot surface as reported with a minor modification [1] was used. In the original proposal, the authors divide the foot surface into 14 regions as shown in Fig. 1(a). Data from T2 to T5 were combined, considering that the device used does not provide information in the individual regions, the combined value provided is denoted by TM. This change generates a smaller division of the foot surface into only 11 regions (Fig.

1(b)).

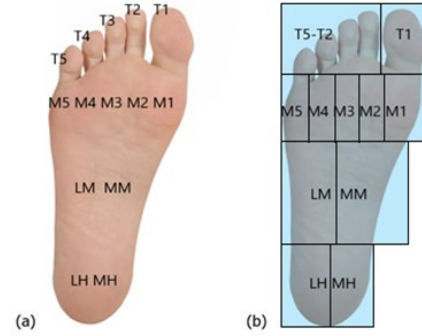


Fig. 1. Main regions on the foot surface: (a) Proposed by [1] where five regions to represent the toes from 1st to 5th (T1–T5), five regions to represent the metatarsal joint from 1st to 5th (M1–M5), and the one region for: the lateral midfoot (LM), the medial midfoot (MM), the lateral heel (LH), and the medial heel (MH). (b) this study, considering the information provided by the device.

The system is based on five stages. In the initial stage, plantar pressure data are acquired by the electronic platform, storage, feature extraction, processing, and the final stage provides foot type classification.

The value of each region defined in the input stage is taken as the percentage load value for each region of the foot surface, which was normalized according to the unit using the weight of each patient, to set each value in the range from 0 to 1. Considering the system variables, the state vector consists of 11 input concepts and 1 output concept. The initial values of the input concepts are the plantar value of each patient, and the initial value of the output concept is set to 0.5 (Fig. 2). This value was defined considering the middle of the range handled by the FCM theory.

In the processing stage, the input concepts are assumed to have an external input with their own weight as described in [18]. Allowing the input variables to remain unchanged, but each auxiliary concept (representing a region of interest of the plantar surface) may be related to each other to represent the behavior of the system, so that all auxiliary concepts (AC) are interconnected. (Fig.3). All AC are set to 0.5 initial value.

During the experimental phase, the FCM formulation (3) showed that the parameter  $k_i$  indicating the influence of the new value on the interconnected concepts had a value close to 1, so this parameter is eliminated and only a part of the value of the past concept is considered, according to following expression:

$$x_i(t) = f\left[\sum_{j \neq i}^n x_j(t-1) W_{ji} + k(x_i(t-1))\right] \quad (5)$$

Where  $k$  is the part between 0 to 1 of the previous concept that is considered to calculate the values of the new concept,  $x_i(t-1)$  is the value of the concept  $C_i$  at time  $t-1$ ,  $W_{ji}$  is the weight matrix,  $x_j(t-1)$  is the value of the concept  $C_j$  at time  $t-1$  and  $f$  is the threshold function (2).

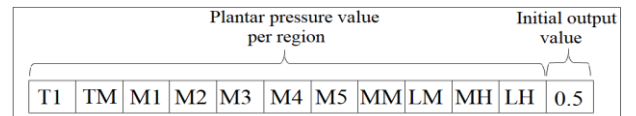


Fig. 2. Encoding schema of concepts.

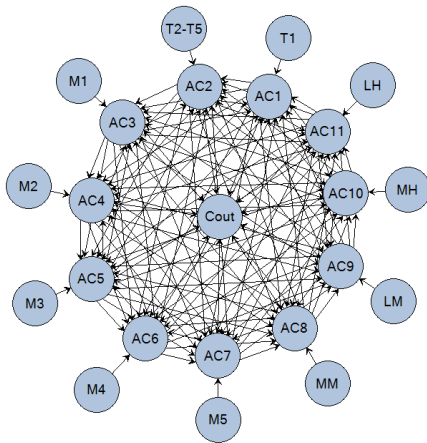


Fig. 3. Graph of the proposed FCM model. External circles mean concepts, internal circles mean auxiliary concepts, and circle in center is the output concept. The arrows represent weighted connections.

Model was evaluated with the bivalent and trivalent threshold functions, but better classification results were obtained with the sigmoid function. Classification results with other threshold functions were not considered in this study, since the objective is to show how FCMs can classify by obtaining potentially transparent systems. To compute the weight matrix interconnecting the concepts and the steepness parameter  $\lambda$  in (2) of the threshold function, a BFOA is used.

The algorithm used has a bacterium representation in which each one is formed by 132 values that compose the FCM weight matrix, a value for the steepness parameter in (2), the iteration number and the constant  $k$  in (5). The optimization algorithm in each iteration tries to find the fittest values to reduce the error function in (6). The algorithm was implemented in C++ using Visual Studio IDE.

$$Error = \sum_{i=1}^n abs(A_i(t) - A_i^p(t)) + abs(SE(t)) \quad (6)$$

where  $n$  is the number of training examples,  $A_i(t)$  is the expected output concept,  $A_i^p(t)$  is the value of the proposed BFOA-FCM concept and  $SE(t)$  is the model stabilization error until a fixed-point attractor is reached, where tolerance threshold  $\varepsilon$  used is 0.01, which means that when two consecutive values  $(t, t + 1)$  differ by less than  $\varepsilon$ , it is considered fixed. This value was obtained considering values between  $[0.01 \text{ to } 0.1]$ .

The error function is satisfied, if the stability of the system and the desired output value is very close to the proposed value ( $\pm 0.01$ ), the values are considered as an acceptable solution; otherwise, the algorithm calculates new parameters for evaluation. The BFOA configuration values are shown in Table I.

In the output stage, to show the result of the foot type classification, a binary encoding is considered, so the output is 1 when the alteration belongs to the class, or 0 when it does not belong to the class.

IV. EXPERIMENTAL RESULTS AND DISCUSSION

A. Performance of the FCM Model

Four FCM models were implemented to obtain a model representing each type of alteration considered. The study included plantar pressure data from 125 subjects with normal ( $n=31$ ), cavus type 3 ( $n=31$ ), cavus type 4 ( $n=31$ ), and flat foot ( $n=32$ ). The proposed model is able to differentiate between what is a specific alteration and what is not.

Graphically, images of alterations considered in this study has the structure shown in Fig. 4 (a-d). The grayscale images in Fig. 4 (e-h) are the views considering the main regions on foot surface. It is clear to note the differences between types. Numerical values of initial state concept vector are summarized in Table II (T1-LH).

Data were normalized to the subject’s weight to obtain each data in a range from 1 to 0. A 5-fold cross-validation was performed on the experiment to obtain more consistent results. The type of alteration was coded to handle it in a computer program. Normal foot is treated as 1, flat foot as 2, cavus foot type 3 as 3, and cavus foot type 4 as 4 (Table II). The weight matrices required by the proposed model and produced by BFOA have a density of 24.95%, which means that 75.05% was not used in all possible connections, to obtain a simpler graph. The model representing each alteration has a different weight matrix, which define the behavior of each system.

During the FCM simulation, the relationship of the concepts produces a behavior between the areas of interest, which change until the FCM simulation reaches a fixed-point attractor.

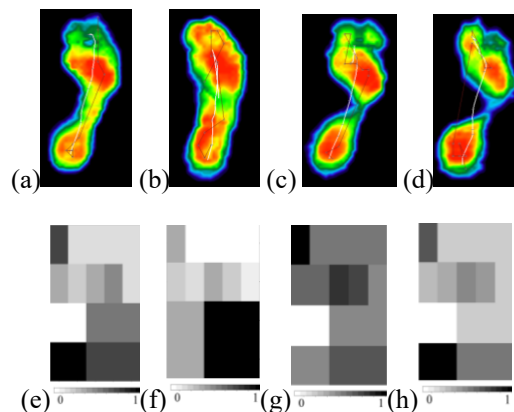


Fig. 4. Shape of the foot surface. (a) Normal foot. (b) Flat foot. (c) Cavus foot type 3. (d) Cavus foot type 4. Main regions on the surface of the foot. (e) Normal foot. (f) Flat foot. (g) Cavus foot type 3. (h) Cavus foot type 4.

TABLE I  
SET-UP VALUES FOR THE BACTERIAL FORAGING OPTIMIZATION ALGORITHM (BFOA)

| Parameter                              | Values    | Final Value |
|--|-----------|-------------|
| Population size                        | 30.0      | 30.0        |
| Number of splits                       | 10-20     | 15.0        |
| Step size                              | 0.01-0.5  | 0.3         |
| Number of elimination-dispersal events | 15-50     | 20.0        |
| Number of reproduction steps           | 5-50      | 10.0        |
| Number of chemotactic steps            | 10-40     | 20.0        |
| Swim length                            | 5-20      | 10.0        |
| Eliminate probability                  | 0.001-0.1 | 0.01        |
| Depth of the attractant                | 1.0-10.0  | 5.0         |
| Width of the attractant signal         | 1.0-10.0  | 5.0         |
| Height of the repellent effect         | 1.0-10.0  | 5.0         |
| Width of the repellent                 | 1.0-20    | 10.0        |

This different behavior for each model allows knowing which areas of interest were considered to converge to the expected result at the time of the simulation, as shown in Fig. 5. This figure shows the behavior of the system when the alteration is present and when it is not present. In the classification results, the FCM simulation reached a fixed-point attractor considering a tolerance threshold  $\epsilon = 0.01$ . Fig. 6 shows the stabilization

behavior of the output concepts for the alterations of randomly chosen subjects from fold 1. For each alteration, it is shown how the system responds, to classify a particular case against the remaining ones. The system stabilizes the simulation at 0 (no alteration) or 1 (alteration exist) before 12 iterations in all cases. Once stability is reached, it allows to obtain the expected result and to compare the behavior between concepts.

TABLE II  
INITIAL STATE CONCEPT VECTOR

| Alteration | Normalized Values |       |       |       |       |       |       |       |       |       |       |       |      |
|------------|-------------------|-------|-------|-------|-------|-------|-------|-------|-------|-------|-------|-------|------|
| ID         | T1                | TM    | M1    | M2    | M3    | M4    | M5    | MM    | LM    | MH    | LH    | AC    | Cout |
|            | C0.1              | C0.2  | C0.3  | C0.4  | C0.5  | C0.6  | C0.7  | C0.8  | C0.9  | C0.10 | C0.11 | C1-11 | C12  |
| 1          | 0.142             | 0.049 | 0.065 | 0.079 | 0.109 | 0.100 | 0.049 | 0.023 | 0.050 | 0.204 | 0.120 | 0.5   | 0.5  |
| 2          | 0.153             | 0.081 | 0.095 | 0.097 | 0.126 | 0.114 | 0.072 | 0.006 | 0.071 | 0.079 | 0.101 | 0.5   | 0.5  |
| 3          | 0.085             | 0.045 | 0.054 | 0.110 | 0.128 | 0.095 | 0.049 | 0.024 | 0.100 | 0.168 | 0.130 | 0.5   | 0.5  |
| 4          | 0.1422            | 0.049 | 0.065 | 0.079 | 0.109 | 0.100 | 0.049 | 0.023 | 0.050 | 0.204 | 0.120 | 0.5   | 0.5  |

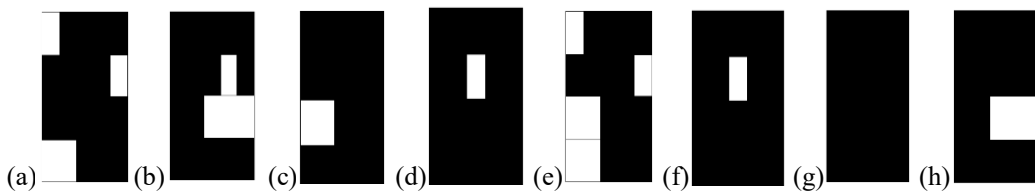


Fig. 5. Behavior of the concepts when a fixed-point attractor is detected for: (a) Flat foot. (b) Cavus foot type 4. (c) Cavus foot type 3. (d) Normal foot. (e) Non-Flat foot. (f) Non-Cavus foot type 4. (g) Non-Cavus foot type 3. (h) Non-normal foot.

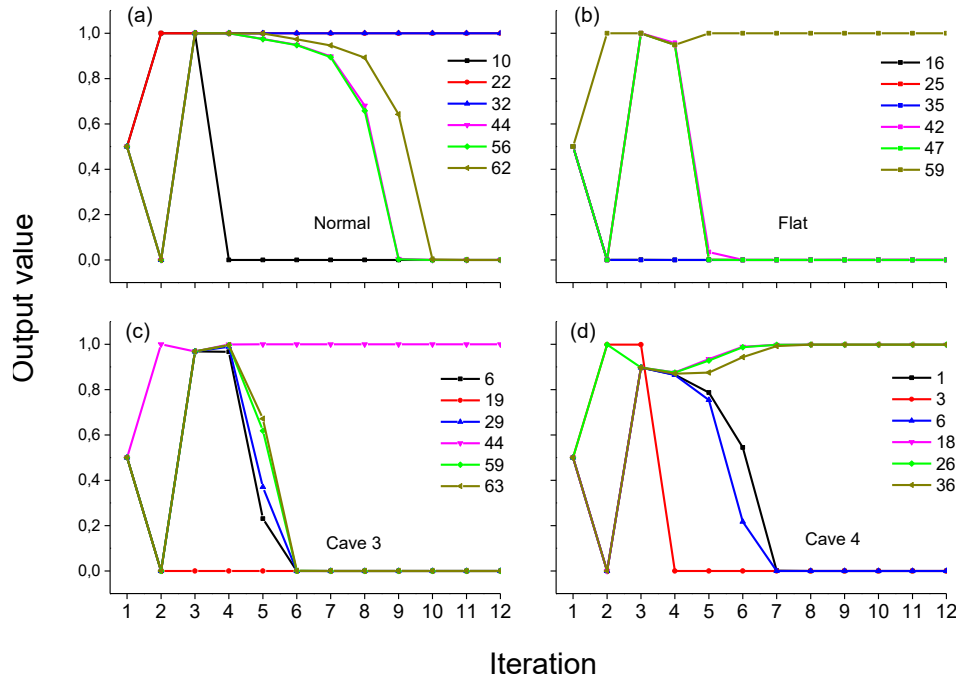


Fig. 6. Subsequent values of output concepts until convergence. Numbers used as labels represent subject number under analysis, chosen randomly from fold 1. (a) Response of Normal foot vs remaining types. (b) Response of Flat foot. vs remaining types. (c) Response of Cavus foot type 3 vs remaining types. (d) Response of Cavus foot type 4 vs remaining types.

The parameter  $\lambda$  in (2), and the number of state vectors were chosen by the optimization algorithm that allows the output to reach a fixed-point efficiently before the 12<sup>th</sup> iteration for alteration (1) and non-alteration (0) avoiding limit cycle and chaotic behavior.

Although stability in an FCM can be reached in a few iterations, it could be noticed that the FCM simulation for the normal foot requires more iterations to reach a fixed point, class where the relationship between the regions is tighter and more difficult to find. For each model representing the foot type, the algorithm found the best solution with different parameters in terms of weight matrix, parameter  $\lambda$  in (2) and constant  $k$  in (5).

**B. Validation of the FCM Model**

Table III shows the classification results of the system in each fold and each alteration, where the arithmetic mean of the evaluation measures was calculated with different partitions, repeating the process 5 times. The training sets had 90% (112 ± 2) of the total data (125) and the rest for the test sets (13 ± 2). The classification error rate with the training data was adjusted around 10% for all the alterations and folds used, as shown in Table III. The probability that the system could correctly classify the test data for each model was adjusted by 89% on average.

The confusion matrices were performed to obtain a more detailed result of the classification task with the proposed method. Table IV shows the average true positives (TP), false positives (FP), false negatives (FN), and true negatives (TN) for the classification task. Table V shows the calculated results, for the average test fold for each alteration.

The BFOA-FCM methodology has a high capacity to detect alterations with an average sensitivity value around 0.93, but the capacity to detect the absence of a specific plantar alteration is lower with an average specificity value around 0.80 (Table V), considering the analysis of the percentage of load per unit area, it is evident that the model has ease in detecting the cavus type 4, due to the absence of load in zones LM and MM. And shows greater difficulty in detecting the normal foot since it has to involve all the areas of interest.

TABLE III  
SCORE FOR EACH FOLD TO CLASSIFY BETWEEN ALTERATIONS

| Type of foot                               | Fold | Score testing data | Average score testing | Average score training |
|--|------|--------------------|-----------------------|------------------------|
| Normal vs non-normal foot                  | 1    | 86.6%              | 83.7%                 | 85%                    |
|  | 2    | 80.6%              |                       |                        |
|  | 3    | 84.3%              |                       |                        |
|  | 4    | 80.4%              |                       |                        |
|  | 5    | 86.6%              |                       |                        |
| Flat vs non-flat foot                      | 1    | 91.1%              | 90.7%                 | 90%                    |
|  | 2    | 93.5%              |                       |                        |
|  | 3    | 96.8%              |                       |                        |
|  | 4    | 90.2%              |                       |                        |
|  | 5    | 82.5%              |                       |                        |
| Cavus foot type 3 vs non-cavus foot type 3 | 1    | 88.8%              | 84.1%                 | 85%                    |
|  | 2    | 80.6%              |                       |                        |
|  | 3    | 81.2%              |                       |                        |
|  | 4    | 80.4%              |                       |                        |
|  | 5    | 89.4%              |                       |                        |
| Cavus foot type 4 vs non-cavus foot type 4 | 1    | 91.1%              | 96.5%                 | 95%                    |
|  | 2    | 100%               |                       |                        |
|  | 3    | 93.7%              |                       |                        |
|  | 4    | 100%               |                       |                        |
|  | 5    | 97.7%              |                       |                        |

TABLE IV  
CONFUSION MATRIX FOR EACH MODEL

|                            | Normal foot                 |                                 |
|----------------------------|-----------------------------|---------------------------------|
|                            | Predicted normal foot       | Predicted non-normal foot       |
| Real normal foot           | 10.6                        | 1.6                             |
| Real non-normal foot       | 6                           | 22.4                            |
|                            | Flat foot                   |                                 |
|                            | Predicted flat foot         | Predicted non-flat foot         |
| Real flat foot             | 8.6                         | 0.4                             |
| Real non-flat foot         | 5                           | 26.6                            |
|                            | Cavus type foot 3           |                                 |
|                            | Predicted cavus foot type 3 | Predicted non-cavus foot type 3 |
| Real cavus foot type 3     | 8.6                         | 0.8                             |
| Real non-cavus foot type 3 | 7.6                         | 24                              |
|                            | Cavus foot type 4           |                                 |
|                            | Predicted cavus foot type 4 | Predicted non-cavus foot type 4 |
| Real cavus foot type 4     | 9.6                         | 0                               |
| Real non-cavus foot type 4 | 3                           | 27.2                            |

TABLE V  
VALIDATION RESULTS IN TERM OF SENSITIVITY, SPECIFICITY AND ACCURACY

| Type of Foot      | Sensitivity | Specificity | Accuracy |
|-------------------|-------------|-------------|----------|
| Normal foot       | 0.86        | 0.78        | 0.81     |
| Flat foot         | 0.95        | 0.84        | 0.86     |
| Cavus foot type 3 | 0.91        | 0.76        | 0.74     |
| Cavus foot type 4 | 1           | 0.78        | 0.92     |

The number of samples was rounded considering the number of samples of the test fold, against the correctly classified samples e.g., a fold of 15 samples, where 13 are correctly classified corresponds to 86.666%.

**C. Comparison of the Model**

To evaluate the methodology used, two physicians manually and individually classified a sample of 50 data from the same database (12 samples of normal foot and flat foot, and 13 samples of cavus foot type 3 and 4 were considered). The results showed that physicians correctly interpreted 60% of normal foot, 75% of flat foot, 50% of cavus foot type 3 and 25% of cavus foot type 4. Each physician classified the different foot types according to their own criteria by viewing the images with pressure levels, as in Fig. 4 (a-d). This classification task is not easy, as confusion can occur when the plantar pressure levels of a subject resemble the two-foot types, where the algorithm was better as it perceives small alterations imperceptible to the human eye. In the presented model, the BFOA-FCM methodology can model the system with the use of an intuitive and small graph, achieving an accuracy of 89%, and it is possible to understand why it makes each classification decision. Previous authors have applied different techniques to use plantar pressure information to detect alterations and provide physicians with useful analysis tools, such as Neural Network and Gaussian Mixture Model (GMM) [9], Fuzzy Cognitive Maps-Genetic algorithm (FCM-GA) and Multi-Layer Perceptron Neural Network (MLPNN) [9]–[11], [27]. Table VI shows the comparison of these previous studies using Fuzzy and non-Fuzzy approaches. Handling different configuration features in the systems, precision rates between

80.9 and 91% have been reported.

TABLE VI  
CLASSIFICATION OF PLANTAR FOOT ALTERATIONS BY DIFFERENT APPROACHES

| Technique      | Reference     | Classification task   | Number of patients       | Parameters of interest  | Feature model | Classification rate |
|----------------|---------------|---|--------------------------|---|---------------|---------------------|
| Neural Network | [9]           | Classifies between normal, diabetic Type 2 with and without neuropathy patients | 84                       | Toe 1st (T1), toe 2nd (T2), toe 3rd to 5th (T3–T5), metatarsal joint 1s (M1), metatarsal joint 2nd (M2), metatarsal joint 3rd to 5th (M3–M5), lateral midfoot (LM), medial midfoot (MM), lateral heel (LH), medial heel (MH). | 20 nodes      | 90.4%               |
| GMM            |               |   |                          |   | -----         | 80.9%               |
| FCM-GA         | [27]          | Classifies between flat and cavus foot  | 151 patients             | Toe 1st, to 5th (T1–T5), metatarsal joint 1st to 5th (M1–M5), lateral midfoot (LM), medial midfoot (MM), lateral heel (LH), medial heel (MH).   | 21 nodes      | 91%                 |
| MLPNN          |               |   |                          |   |               | 87%                 |
| BFOA-FCM       | Applied model | Classifies between normal, flat, cavus type 3 and cavus type 4 foot             | 250 feet of 125 patients | Toe 1st, toe 2nd to 5th (T2–T5), metatarsal joint 1st to 5th (M1–M5), lateral midfoot (LM), medial midfoot (MM), lateral heel (LH), medial heel (MH).   | 23 nodes      | 89%                 |
| Physician      | Applied study | Classifies between normal, flat, cavus type 3 and cavus type 4 foot             | 50 feet of patients      | Toe 1st, toe 2nd to 5th (T2–T5), metatarsal joint 1st to 5th (M1–M5), lateral midfoot (LM), medial midfoot (MM), lateral heel (LH), medial heel (MH).   | Manual        | 52.5%               |

BFOA-FCM approach uses 23 nodes each with understandable meaning, avoiding black boxes in the operation.

Compared to the study of similar experimental features [27], where a high rate of success in the global classification was achieved, the number of classes was lower. So as more classes are included, the pattern becomes more difficult to find because the differences that identify them are more refined. With the proposed methodology for the classification of flat and cavus foot, it has been achieved up to 100% success in the classification, but by including the other classes the overall classification rate decreases because it becomes more complicated processing and classification. It is necessary to build a more complete database, with the integration of more knowledge sources and more samples in order to have a larger amount of data for training and for testing, so as to improve the learning of the algorithm.

## V. CONCLUSION

The classification task of orthopedic foot alterations is not simple, as more possible classification groups (Normal, flat, type 3 cavus, type 4 cavus, etc.) may lead to confusion in the final decision making. The foot pattern varies between subjects, making it difficult to detect small differences that make the result an alteration or another.

The FCM with BFOA proves to be a useful methodology, since through a simple structure and using an effective decision mechanism similar to that of humans, it is possible to classify with results close to 89% and to know the interaction between regions, which the system took into account to achieve the result. On the other hand, the response of the system is stable, where the number of iterations to reach the fixed point attractor varies between foot types as the difficulty to find the pattern varies. The model obtained is simple with only 11 input nodes representing each region of interest of the plantar surface as a function of the load percentage; 11 auxiliary nodes proposed to improve the performance of the graph and to observe the relationship between the input concepts; and one output node

that allows classifying between what is an alteration and what is not. This type of classification output works as a filter, where with a new patient, the plantar pressure data must be tested with the 4 matrices.

The precision and accuracy of the system change in relation to the number of foot types to be identified. As more types exist to classify, become more difficult to find the pattern. It was possible to obtain a classification result close to 90% that may be improved by using another optimization algorithm or a variation in the number of regions of interest on the plantar surface. To improve the results, further studies are being carried out considering a larger group of specialists to study populations from different countries with similar morphological characteristics. Also, the inclusion of postural variables can help the proposed algorithm to make a decision with greater accuracy and precision.

## AGRADECIMIENTOS

This work was supported in part by Centro de Investigación en Ciencia Aplicada y Tecnología Avanzada, Querétaro unit, from Instituto Politécnico Nacional, México; Consejo Nacional de Ciencia y Tecnología (CONACyT), México; PIEDICA center, México; BASPI-FootLaB, Electronic Department, from Pontificia Universidad Javeriana, Colombia; Universidad Autónoma de Querétaro, México; and Fundación Universitaria de San Gil – UNISANGIL, Colombia. (Corresponding author: J. A. Ramirez).

## REFERENCES

- [1] J. A. R. Bautista, S. L. C. Cárdenas, A. H. Zavala, and J. A. Huerta-Ruelas, "Review on plantar data analysis for disease diagnosis," *Biocybern. Biomed. Eng.*, vol. 8, 2018.
- [2] J. A. Ramirez-Bautista, J. A. Huerta-Ruelas, S. L. Chaparro-Cardenas, and A. Hernandez-Zavala, "A Review in Detection and Monitoring Gait Disorders Using In-Shoe Plantar Measurement Systems," *IEEE Rev. Biomed. Eng.*, vol. 10, no. c, pp. 299–309, 2017.
- [3] S. Kundu, U. S. Acharya, and S. Mukherjee, *Proceedings of the 2nd International Conference on Communication, Devices and Computing*,

- vol. 602. Singapore: Springer Singapore, 2020.
- [4] D. R. Bonanno, K. Ledchumanasarma, K. B. Landorf, S. E. Munteanu, G. S. Murley, and H. B. Menz, "Effects of a contoured foot orthosis and flat insole on plantar pressure and tibial acceleration while walking in defence boots," *Sci. Rep.*, vol. 9, no. 1, p. 1688, Dec. 2019.
  - [5] J. A. Ramirez-Bautista, J. A. Huerta-Ruelas, S. L. Chaparro-Cárdenas, and A. Hernández-Zavala, "A Review in Detection and Monitoring Gait Disorders Using In-Shoe Plantar Measurement Systems," *IEEE Reviews in Biomedical Engineering*, vol. 10, pp. 299–309, 2017.
  - [6] J. Chae, Y.-J. Kang, and Y. Noh, "A Deep-Learning Approach for Foot-Type Classification Using Heterogeneous Pressure Data," *Sensors*, vol. 20, no. 16, p. 4481, Aug. 2020.
  - [7] D. A. Pelta, C. Cruz, A. D. Masegosa, E. Onieva, P. Lopez-garcia, and E. Osaba, *Soft Computing Based Optimization and Decision Models*, Springer I., vol. 360. Cham: Springer International Publishing, 2018.
  - [8] S. Sujamol, S. Ashok, and U. K. Kumar, "Study of Fuzzy Cognitive Maps for Modeling Clinical Support Systems," *Int. J. Pure Appl. Math.*, vol. 119, no. 12, pp. 15433–15445, 2018.
  - [9] R. Acharya U *et al.*, "Automated Identification of Diabetic Type 2 Subjects with and without Neuropathy Using Wavelet Transform on Pedobarograph," *J. Med. Syst.*, vol. 32, no. 1, pp. 21–29, Feb. 2008.
  - [10] H. Li *et al.*, "Modified Weights-and-Structure-Determination Neural Network for Pattern Classification of Flatfoot," *IEEE Access*, vol. 7, pp. 63146–63154, 2019.
  - [11] S. Xu, X. Zhou, and Y.-N. Sun, "A novel gait analysis system based on adaptive neuro-fuzzy inference system," *Expert Syst. Appl.*, vol. 37, no. 2, pp. 1265–1269, Mar. 2010.
  - [12] Z. Mei, K. Ivanov, G. Zhao, Y. Wu, M. Liu, and L. Wang, "Foot type classification using sensor-enabled footwear and 1D-CNN," *Meas. J. Int. Meas. Confed.*, vol. 165, p. 108184, Dec. 2020.
  - [13] J. Han, D. Wang, Z. Li, N. Dey, R. G. Crespo, and F. Shi, "Plantar pressure image classification employing residual-network model-based conditional generative adversarial networks: a comparison of normal, planus, and talipes equinovarus feet," *Soft Comput.*, pp. 1–20, Aug. 2021.
  - [14] D. A. Pelta and C. Cruz, "Soft Computing Based Optimization and Decision Models", Springer I., vol. 360. Cham: Springer International Publishing, 2018.
  - [15] E. Vayena, A. Blasimme, and I. G. Cohen, "Machine learning in medicine: Addressing ethical challenges," *PLOS Med.*, vol. 15, no. 11, p. e1002689, Nov. 2018.
  - [16] A. Amirkhani, E. I. Papageorgiou, A. Mohseni, and M. R. Mosavi, "A review of fuzzy cognitive maps in medicine: Taxonomy, methods, and applications," *Comput. Methods Programs Biomed.*, vol. 142, pp. 129–145, Apr. 2017.
  - [17] E. I. Papageorgiou and J. L. Salmeron, "A Review of Fuzzy Cognitive Maps Research During the Last Decade," *IEEE Trans. Fuzzy Syst.*, vol. 21, no. 1, pp. 66–79, Feb. 2013.
  - [18] C. D. Stylios and P. P. Groumpos, "Mathematical formulation of fuzzy cognitive maps," *Proc. 7th Mediterr. Conf. Control Autom.*, June 1999, pp. 2251–2261.
  - [19] G. Papakostas and D. E. Koulouriotis, "Classifying Patterns Using Fuzzy Cognitive Maps," in *Fuzzy cognitive maps*, 2010, vol. 247, pp. 291–306.
  - [20] S. Ahmadi, N. Forouzideh, C. H. Yeh, R. Martin, and E. Papageorgiou, "A first study of Fuzzy Cognitive Maps learning using cultural algorithm," in *Proceedings of the 2014 9th IEEE Conference on Industrial Electronics and Applications, ICIEA 2014*, 2014, pp. 2023–2028.
  - [21] C. D. Stylios, V. C. Georgopoulos, G. A. Malandraki, and S. Chouliara, "Fuzzy cognitive map architectures for medical decision support systems," *Appl. Soft Comput.*, vol. 8, no. 3, pp. 1243–1251, Jun. 2008.
  - [22] P. P. Groumpos and A. P. Anninou, "A theoretical mathematical modeling of Parkinson's disease using Fuzzy Cognitive Maps," in *2012 IEEE 12th International Conference on Bioinformatics & Bioengineering (BIBE)*, Nov. 2012, no. November, pp. 677–682.
  - [23] E. I. Papageorgiou, C. D. Stylios, and P. P. Groumpos, "An integrated two-level hierarchical system for decision making in radiation therapy based on fuzzy cognitive maps," *IEEE Trans. Biomed. Eng.*, vol. 50, no. 12, pp. 1326–1339, Dec. 2003.
  - [24] P. Oikonomou and E. I. Papageorgiou, "Particle Swarm Optimization Approach for Fuzzy Cognitive Maps Applied to Autism Classification," in *IFIP Advances in Information and Communication Technology*, vol. 412, IFIP International Federation for Information Processing, 2013, pp. 516–526.
  - [25] M. Khodadadi, H. Shayanfar, K. Maghooli, and A. H. Mazinan, "Prediction of stroke probability occurrence based on fuzzy cognitive maps," *Automatika*, vol. 60, no. 4, pp. 385–392, Oct. 2019.
  - [26] V. K. Mago, R. Mehta, R. Woolrych, and E. I. Papageorgiou, "Supporting meningitis diagnosis amongst infants and children through the use of fuzzy cognitive mapping," *BMC Med. Inform. Decis. Mak.*, vol. 12, no. 1, p. 98, Dec. 2012.
  - [27] J. A. Ramirez-Bautista, J. A. Huerta-Ruelas, L. T. Kóczy, M. F. Hatwagner, S. L. Chaparro-Cárdenas, and A. Hernández-Zavala, "Classification of plantar foot alterations by fuzzy cognitive maps against multi-layer perceptron neural network," *Biocybern. Biomed. Eng.*, vol. 40, no. 1, pp. 404–414, 2020.
  - [28] B. Kosko, "Fuzzy cognitive maps," *Int. J. Man. Mach. Stud.*, vol. 24, no. 1, pp. 65–75, Jan. 1986.
  - [29] G. A. Papakostas, Y. S. Boutalis, D. E. Koulouriotis, and B. G. Mertzios, "Fuzzy cognitive maps for pattern recognition applications," *Int. J. Pattern Recognit. Artif. Intell.*, vol. 22, no. 8, pp. 1461–1486, Dec. 2008.
  - [30] M. F. Hatwagner, V. A. Niskanen, and L. T. Kóczy, "Behavioral analysis of fuzzy cognitive map models by simulation," *IFSA-SCIS 2017 - Jt. 17th World Congr. Int. Fuzzy Syst. Assoc. 9th Int. Conf. Soft Comput. Intell. Syst.*, 2017.
  - [31] G. Nápoles *et al.*, "Fuzzy cognitive modeling: Theoretical and practical considerations," in *Smart Innovation, Systems and Technologies*, vol. 142, no. June, 2019, pp. 77–87.
  - [32] M. F. Hatwagner, G. Vastag, V. A. Niskanen, and L. T. Kóczy, "Banking applications of FCM models," *Springer-Verlag*, pp. 1–9, 2011.
  - [33] E. I. Papageorgiou, "Learning Algorithms for Fuzzy Cognitive Maps—A Review Study," *IEEE Trans. Syst. Man, Cybern. Part C (Applications Rev.)*, vol. 42, no. 2, pp. 150–163, Mar. 2012.
  - [34] G. Felix, G. Nápoles, R. Falcon, W. Froelich, K. Vanhoof, and R. Bello, "A review on methods and software for fuzzy cognitive maps," *Artif. Intell. Rev.*, vol. 52, no. 3, pp. 1707–1737, Oct. 2019.
  - [35] G. A. Papakostas, D. E. Koulouriotis, A. S. Polydoros, and V. D. Tourassis, "Towards Hebbian learning of Fuzzy Cognitive Maps in pattern classification problems," *Expert Syst. Appl.*, vol. 39, no. 12, pp. 10620–10629, Sep. 2012.
  - [36] E. I. Papageorgiou, C. D. Stylios, and P. P. Groumpos, "Active Hebbian learning algorithm to train fuzzy cognitive maps," *Int. J. Approx. Reason.*, vol. 37, no. 3, pp. 219–249, Nov. 2004.
  - [37] C. D. Stylios and V. C. Georgopoulos, "Genetic algorithm enhanced Fuzzy Cognitive Maps for medical diagnosis," in *2008 IEEE International Conference on Fuzzy Systems (IEEE World Congress on Computational Intelligence)*, Jun. 2008, pp. 2123–2128.
  - [38] K. M. Passino, "Biomimicry of bacterial foraging for distributed optimization and control," *IEEE Control Syst.*, vol. 22, no. 3, pp. 52–67, Jun. 2002.
  - [39] B. Hernandez-Ocana, E. Mezura-Montes, and P. Pozos-Parra, "A review of the bacterial foraging algorithm in constrained numerical optimization," *2013 IEEE Congr. Evol. Comput. CEC 2013*, pp. 2695–2702, 2013.
  - [40] K. M. Passino, "Bacterial Foraging Optimization," *Int. J. Swarm Intell. Res.*, vol. 1, no. 1, pp. 1–16, Jan. 2010.
  - [41] N. K. Jhankal and D. Adhyaru, "Comparative Analysis of Bacterial Foraging Optimization Algorithm with Simulated Annealing," *Int. J. Sci. Res.*, vol. 3, no. 3, pp. 10–13, 2014.
  - [42] S. Das, A. Biswas, S. Dasgupta, and A. Abraham, "Bacterial Foraging Optimization Algorithm: Theoretical Foundations, Analysis, and Applications," pp. 23–55, 2009.



**J. A. Ramirez-Bautista.** Electronic Engineer from the Fundación Universitaria de San Gil (UNISANGIL), San Gil, Colombia, in 2013. The master degree in advanced technology, and the Ph.D. degree in advanced technology, with a specialty in mechatronics, from the Research Center for Applied Science and Advanced Technology (CICATA), Instituto Politécnico Nacional, Queretaro, Mexico, in 2016 and 2020. His research interests include fuzzy systems, hybrid systems, interface development, neural networks, and clinical decision support systems. He is currently a full-time professor at the Faculty of Natural Sciences and Engineering of UNISANGIL,



**S.L. Chaparro-Cárdenas.** Electronic Engineer from the Fundación Universitaria de San Gil (UNISANGIL), San Gil, Colombia, in 2013. The master degree in advanced technology, and the Ph.D. degree in advanced technology, with a specialty in mechatronics, from the Research Center for Applied Science and Advanced Technology (CICATA), Instituto Politécnico Nacional, Queretaro, Mexico, in 2016 and 2021. She is currently a professor and researcher in UNISANGIL, Colombia. Her research interests include fuzzy systems, hybrid systems, robotic rehabilitation devices, neural networks, intelligent control and electrophysiology.



**A. Hernández-Zavala.** Received the Computer Systems engineer title from the Tecnológico de Estudios Superiores de Ecatepec, México, in 2001. Received the Master degree in computer engineering with a specialty in digital systems in 2004 and the Ph. D degree in computer architecture in 2009, both from the Centro de Investigación en Computación from Instituto Politécnico Nacional, México. Currently, he is a member of the National Researchers System (SNI) and is a full-time professor at Mechatronics department in Centro de Investigación en Ciencia Aplicada y Tecnología Avanzada CICATA from IPN, in Querétaro city. His research interests include Fuzzy Logic, Fuzzy Hardware, Fuzzy Control, Neural Networks, Computer Architecture, and Digital Logics.



**R. M. Gallegos-Torres.** Bachelor's Degree in Nursing from the Universidad Veracruzana, Master's Degree in Nursing Sciences and Doctor in Health Sciences from the Universidad Autónoma de Querétaro. Specialty in Drug Phenomenon Research in Toronto, Canada. Multiple courses and diplomas in research. More than 70 publications in scientific journals and national and international papers. She has been conducting research for more than 23 years. Since 2008, she has been teaching research subjects at undergraduate and graduate level. She has directed multiple undergraduate and master's theses. Full-time professor since 2006 of the Faculty of Nursing at the Autonomous University of Queretaro. Certified as a teacher by the Mexican Council for Nursing Certification.



**M. Zequera.** Obtained her MSc in Biomedical Engineering at the University of Dundee, UK, in 1992 and her PhD from the Bioengineering Unit of the University of Strathclyde, UK, in 2003. Since 2010 she is an Honorary Research Fellow of the University of Strathclyde in the Bioengineering Unit, United Kingdom. Prof. Zequera is Full Professor in the Electronics Department of

the Faculty of Engineering, at the Pontificia Universidad Javeriana, Bogotá, Columbia since 2010. She has been working as a researcher for 24 years in the Bioengineering Research Group "BASPI", oriented to biosignal and image processing analysis. Her current research interests include the integration of emerging technologies and the analysis of information with the use of deep learning techniques for the prediction of neurological diseases in elderly patients with diabetes.



**Y. Tovar-Barrera.** Bachelor in Physical Therapy graduated from the Polytechnic University of Santa Rosa Jauregui (UPSRJ), in Queretaro Mexico, in 2016. He performed his social service at the Hospital General Naval de Alta Especialidad (HOSGENAES) 2015-2016. Worked in the Integral Development System for the family (DIF) of Tequisquiapan, (2017-2020). In 2018 he completed a certification in Manual Therapy of Cervicalgias and Neuralgias and Cervicobrachial. In 2019 he completed a certificate in Neurodianamia. In 2020 he completed a certification in recommendations for a safe return to work before the COVID-19. In 2021 he completed a certification in low back pain. He currently works at Yosafisio Clinic.



**J. M. Pradilla-Gómez.** Professional doctor from the Pontificia Universidad Javeriana born in Bucaramanga – Colombia and studied in Bogotá - Colombia, with a high sense of commitment currently working as a surgical assistant in Orthopedics and as doctor of the hospital area of the orthopedic service in two different renowned institutions (Clinica La Sabana and Fundacion Cardioinfantil) in the city of Bogotá. He constantly maintains the willingness to acquire academic and professional concepts participating in multiples symposia and congresses, in addition to the desire to continue developing research in the area by contributing to publication related to the area of orthopedic. Also, he has a high sense of responsibility and humanity by being volunteer in programs of charity in his country as (TECHO).



**J. A. Huerta-Ruelas.** Received the Master of Science degree in solid state physics and the Ph.D. degree in electrical engineering from the Autonomous University of San Luis Potosi, San Luis Potosi, Mexico, in 1995 and 2000, respectively. He held a Postdoctoral Fellowship in the Department of Science and Food Technology, Oregon State University, Corvallis, OR, USA, in 2004. He is a Professor with the Advanced Technology Graduate Program, teaching: optical characterization techniques, interaction of radiation with matter, and the writing and publishing of technical and scientific documents. He is currently a member of the National System of Researchers. His current research focuses on the development of optical measuring systems for use in research and industrial process control, that includes instrumentation, optomechanical design, and programming.